AMAZONIAN GLACIATION IN EASTERN HELLAS, MARS: EVIDENCE FOR HIGH-ALTITUDE ATMOSPHERIC DEPOSITION AS THE SOURCE FOR THE HOURGLASS AND RELATED DEPOSITS.

J. L. Dickson[1] and J. W. Head[1], [1]Brown University, Dept. Geo. Sci., Providence, RI, 02912 (jdickson@brown.edu).

Introduction: Several major regions of Mars have been significantly modified in the Late Amazonian by features interpreted to have formed by ice-assisted creep [1,5] or glacial-like flow [2-4, 6-8]. These regions are found where high-resolution climate simulations of Mars at higher obliquity predict the greatest accumulation of snow and ice [9, 10]: The western flanks of the Tharsis Montes [4], the dichotomy boundary north of Arabia [7-8], and eastern Hellas [5-6]. The eastern Hellas region has been studied in detail using Mars Global Surveyor [5] and Mars Express (MEX) [6] data and is a potential area of deposition for volatiles transported from the south polar cap [9].

Eastern Hellas (Fig. 1, centered at 39°S, 102°E) is comprised of large massifs and mountains interspersed among regionally smooth, softened plains. The massifs display lobate, concentric aprons on their flanks that have been interpreted as remnants of debris-covered cold-based glaciers in the Late Amazonian [6]. The wide spatial coverage of the High Resolution Stereo Camera (HRSC) on MEX revealed one of these deposits to be in the geometry of an hourglass (Fig. 2), where ice was interpreted to have collected in accumulation zones near the base of a massif underwent flow into a crater, convergence and constriction, then expanding into a larger crater [6]. While agreeing with the broad piedmont-glacial model, other workers disputed the interpretation that the ice was atmospherically derived, arguing that the most recent phase of glaciation in the craters was sourced by groundwater erupting from exposed aquifers [11].

Here, we use new Mars Reconnaisance Orbiter CTX data to document the most recent glacial activity which is seen to be areally continuous from the higher elevations of the neighboring massif to the floor of the hourglass double-crater system. We then analyze new data from a neighboring double-crater system with a similar set of hourglass-shaped glacial deposits, and we argue for the past existence of ice thicker than the deposits presently observed on the surface.

Sources for the most recent glaciation: Head et al. [6] mapped four accumulation zones along the northern, eastern and southern margins of the eastern crater in the hourglass orientation (Fig. 1-3). Of these four, the most distinctive zone is found in the southeastern portion of the crater. The flow on the floor in the proximal zone is characterized by concentric lobate margins, 2 km wide at maximum width, emanating from the massif flanks (Fig. 2-3).

Several CTX orbits have targeted this feature at ~6 m/px, revealing details of surface texture that were previously unavailable (Fig. 3). A detailed study of the terrain on the massif up slope from this zone of flow shows streamlined ridges indicative of viscous flow; these are the source for this most recent phase of glacial activity (Fig. 3). These features can be traced back for 12 km to a region of tributary glaciers that appear to have coalesced and flowed south to source the hourglass glacial deposits.

This upslope accumulation zone occurs at a topographic divide: ice that accumulated south of this zone flowed to the south and contributed to the massive 27 km wide lobe seen in Fig. 4. This major accumulation zone occurs at ~3100 m elevation, well above the regional plains, making groundwater an unlikely source. We interpret the surface morphology and topographic and stratigraphic relationships to mean that the most recent phase of glaciation in this region was sourced by atmospheric precipitation [9] that accumulated, coalesced, and formed glaciers that flowed downslope to the north and the south [9].

Evidence for previous vertical extent: A similar hourglass geometry for a double-crater system is observed just ~35 km to the north of the previously documented system (Fig. 1). Unlike the first hourglass system, flow between the two craters is not continuous in the present-day deposits, and the two craters are separated by a narrow ridge (Fig. 5). In the southern of the two craters, remnant flow patterns show that flow was from northeast to southwest, with the distal deposits abutting the wall of the crater. We interpret this geometry to mean that the northern, larger crater was once filled with ice to such an extent that the dividing ridge between the craters was overtopped and flow into the southern crater occurred. Eventually, as accumulation decreased, the ice downwasted, flow between the two craters ceased, and the dividing ridge was exhumed by sublimation. This altered the flow regime, and the waning stages of glacial activity were controlled by the local topography within each crater, causing largely centripetal flow.

Evidence for a former highstand of ice nearly a kilometer above current LDA/LDF has been found along the dichotomy boundary [12, 13]. In eastern Hellas, the ridge that divides the two craters similarly implies a previously much greater thickness of ice than simply reflected by the deposits today.

References: [1] Squyres, S.W., (1978) *Icarus, 34*, 600-613. [2] Lucchitta, B.K., (1981) *Icarus, 45,* 264-303. [3] Lucchitta,

B.K., (1984) *J. Geophys. Res., LPSC Proc. XIV*, B409-B418. [4] Head, J.W. and D.R. Marchant, (2003) *Geology, 31,* 641. [5] Pierce, T.L. and D.A. Crown, (2003), *Icarus, 163,* 46-65. [6] Head, J.W., et al., (2005) *Nature, 434,* 346-351. [7] Head, J.W., et al., (2006a) *EPSL, 241,* 663-671. [8] Head, J.W., et al., (2006) *Geophys. Res. Lett., 33,* 10.1029/2005GL024360. [9] Forget, F., et al., (2006) *Science, 311,* 368-371. [10] Madeleine, J.-B., et al., (2007) *7th Mars*, #3096. [11] Gillespie, A.R., et al., (2005) *Nature, 438,* E9-E10, doi: 10.1038/nature04357. [12] Dickson, J.L., et al., (2008), *Geology*, in revision. [13] Head, J.W., *46th Brown/Vernadsky Microsymposium,* abstract m46_24.

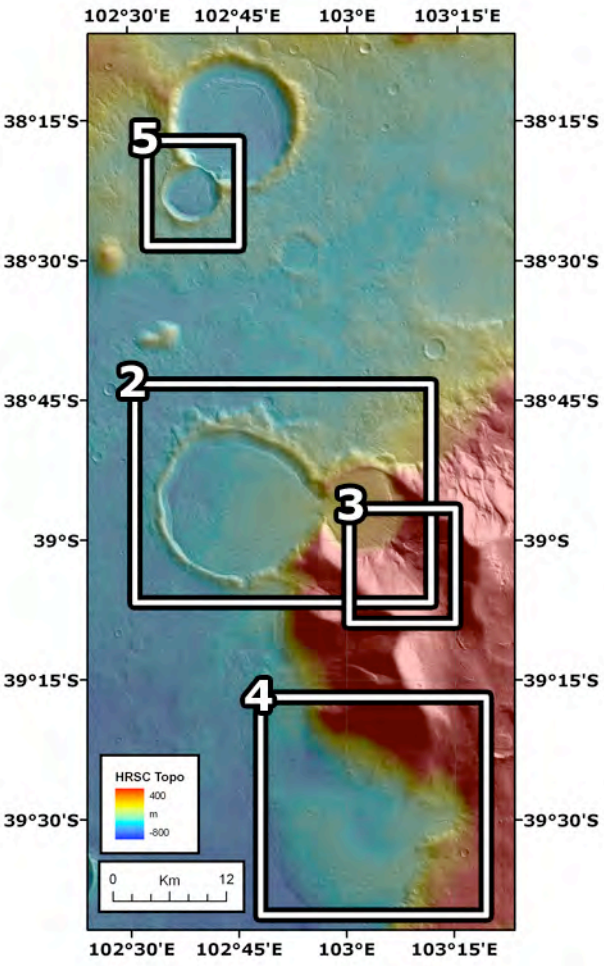

Figure 1. HRSC stereo topography (orbit h0451_0000) over HRSC visible data (orbit h0451_0000).

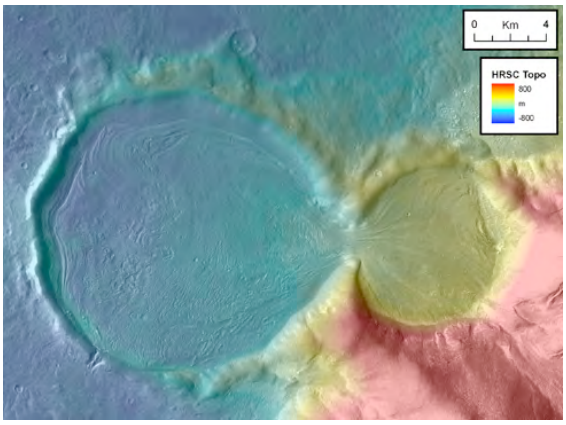

Figure 2. HRSC topography (orbit h0451_0000) over CTX visible data (P05_002782_1407).

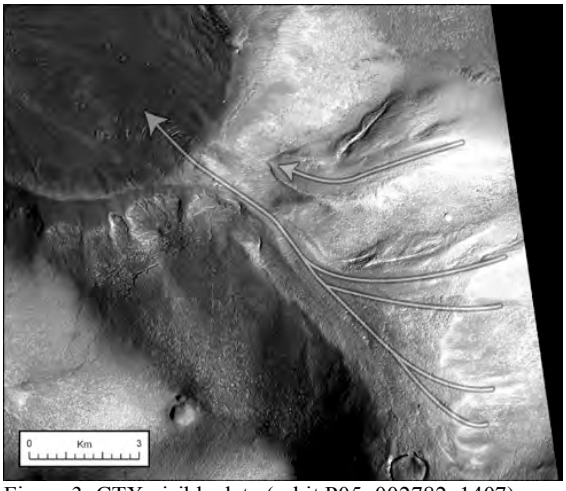

Figure 3. CTX visible data (orbit P05_002782_1407). Arrows represent observed flow patterns.

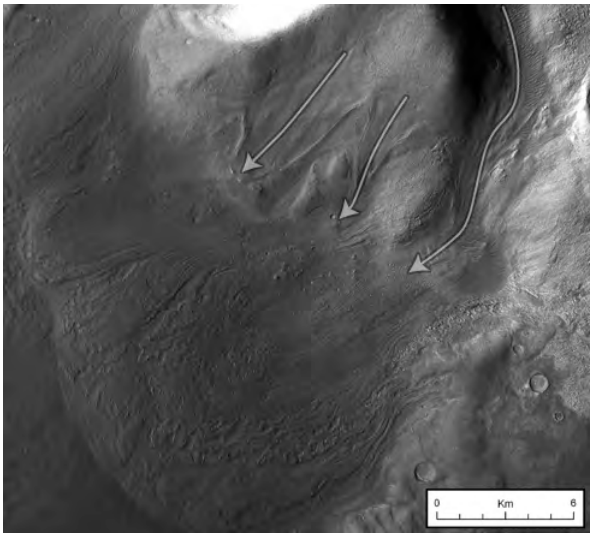

Figure 4. CTX visible data (orbit P03_002148_1409). Arrows represent observed flow patterns

Figure 5. CTX visible data (orbit P05_002782_1407).